

# The Preliminary Study of the 4 March 2010 $M_w$ 6.3 Jiasian, Taiwan Earthquake Sequence

Hsin-Hua Huang<sup>1</sup>, Yih-Min Wu<sup>1\*</sup>, Ting-Li Lin<sup>1</sup>, Wei-An Chao<sup>1</sup>, J. Bruce H. Shyu<sup>1</sup>, Chung-Han Chan<sup>1</sup>, and Chien-Hsin Chang<sup>2</sup>

<sup>1</sup>Department of Geosciences, National Taiwan University, Taipei, Taiwan

<sup>2</sup>Central Weather Bureau, Taipei, Taiwan

Received 9 August 2010, accepted 13 December 2010

---

## ABSTRACT

On 4 March 2010, an inland  $M_w$  6.3 earthquake occurred near the town of Jiasian in Kaohsiung County, Taiwan causing large ground shaking and extensive damage. In this study, we integrate the records from the Central Weather Bureau Seismic Network (CWBSN) and Taiwan Strong Motion Instrumentation Program (TSMIP) to obtain the relocated earthquake sequence and its first-motion focal mechanisms. This dataset offers us precise and reliable results which suggest a focal depth of 23 km and a possible fault plane of strike  $313^\circ$ , dip  $41^\circ$ , and rake  $42^\circ$  for the Jiasian earthquake. This fault plane significantly differs from the N-S striking Chaochou Fault (CCF) as well as the principal trend of Taiwan orogenic belt, and should be an undiscovered fault in southern Taiwan. The relocated Jiasian earthquake sequence initiating from the 23-km-deep mainshock and terminating at around 10 km in depth also indicates it is a blind fault. Peak ground acceleration (PGA) and peak ground velocity (PGV) recorded by the TSMIP stations reveal a distinct NW-SE-shape pattern from the epicenter area toward the Chiayi region, likely due to the directivity and site effects. Such phenomena should be considered for future regional hazard assessments.

Key words: Earthquake, Damage earthquake, Strong ground motion, Focal mechanism

Citation: Huang, H. H., Y. M. Wu, T. L. Lin, W. A. Chao, J. B. H. Shyu, C. H. Chan, and C. H. Chang, 2011: The preliminary study of the 4 March 2010  $M_w$  6.3 Jiasian, Taiwan earthquake sequence. *Terr. Atmos. Ocean. Sci.*, 22, 283-290, doi: 10.3319/TAO.2010.12.13.01(T)

---

## 1. INTRODUCTION

On 4 March 2010, an inland shallow earthquake ( $M_L = 6.4$  and  $M_w = 6.3$ ) near the town of Jiasian in Kaohsiung County, Taiwan, was reported by the Central Weather Bureau (CWB) rapid reporting system (Wu et al. 1997, 2002) and named the “2010 Jiasian earthquake” (Fig. 1). It produced widespread strong ground shaking in southern Taiwan. The maximum PGA up to 475 gal was recorded by station MTN154 of TSMIP with the epicentral distance of about 8 km, and most regions with epicentral distances less than 50 km recorded PGA greater than 250 gal (CWB Intensity scale V, Wu et al. 2003a; Fig. 2a). Hence, this event produced extensive damage such as the collapse of one bridge, fires at five factories and schools, interruption of the regional power grid (which affected 540000 households), damage

to hundreds of buildings, derailment of a high-speed train, and injury to 96 people (National Fire Agency News Release 2010). Several surface cracks were also observed and reported sequentially around the epicenter area (Chang et al. 2010). After decades of seismic silence since the 1964  $M_L = 6.3$  Paiho earthquake, this earthquake awakened people to the potential for the occurrence of destructive earthquake in southern Taiwan.

The N-S striking CCF was initially considered as the causative fault of this event due to its proximity to the epicenter and the shallow focal depth of 5 km as reported by the CWB rapid reporting system using a half-space model with a linear increasing of velocity in depth and automated location process. The Global Centroid Moment Tensor (GCMT), Broadband Array in Taiwan for Seismology (BATS), and CWB using waveform modeling derive similar results of focal mechanism, and suggest two nodal planes: one strikes nearly N-S and the other strikes NW-SE

---

\* Corresponding author  
E-mail: drymwu@ntu.edu.tw

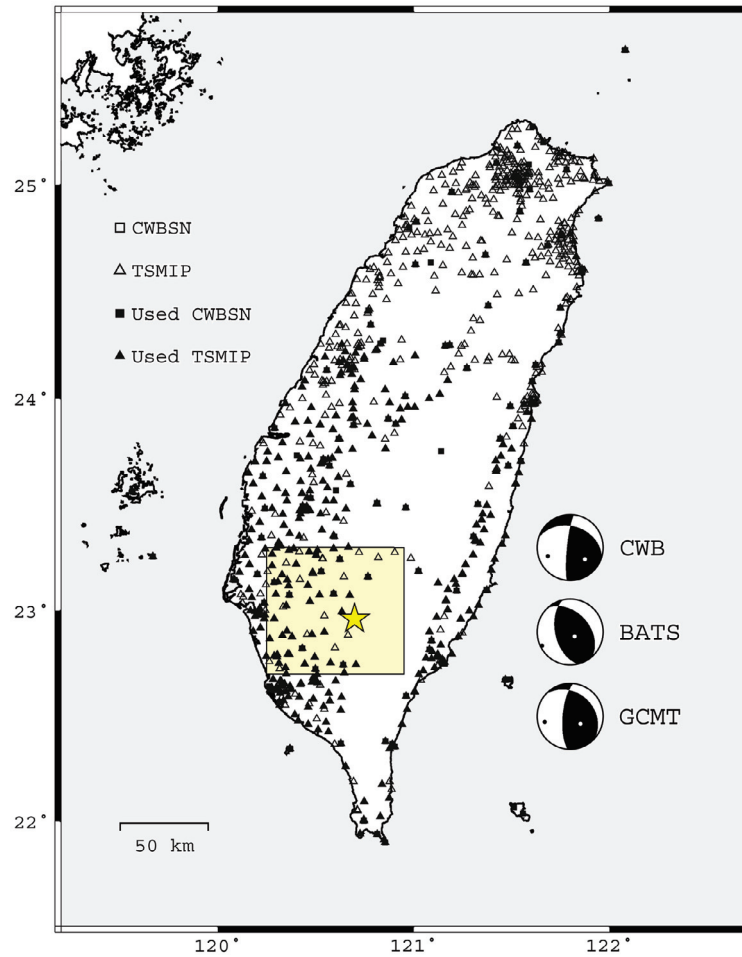


Fig. 1. Station distribution of the CWBSN and TSMIP are denoted by squares and triangles, respectively, while the solid ones indicate the stations used in this study. The star shows the epicenter of the Jiasian earthquake. Its focal mechanisms derived from CWB, BATS, and GCMT are also shown. The shadowed area represents the study area in Figs. 3 and 5, bounded by longitudes 120.25 to 120.95°E, and latitudes 22.7 to 23.3°N.

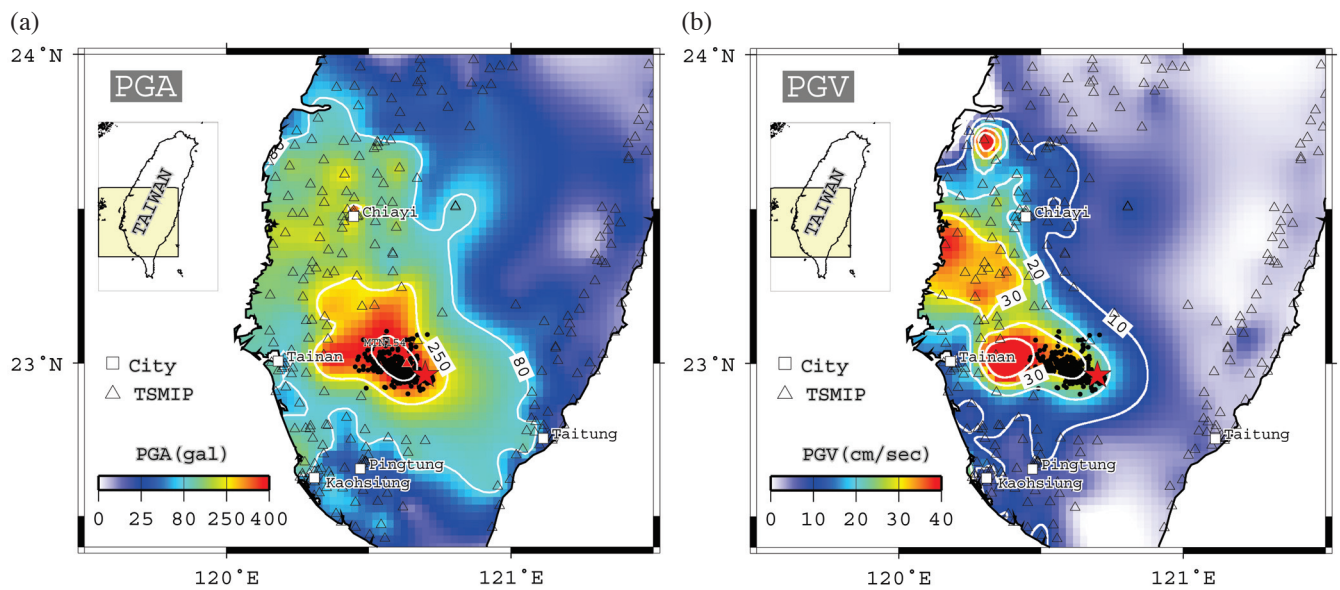


Fig. 2. Distributions of (a) PGA and (b) PGV caused by the 2010 Jiasian earthquake. The open triangles represent the stations of TSMIP. The red triangle in (a) shows the location of station MTN154 that recorded the maximum PGA to 475 gal. The solid circles show the 474 aftershocks occurred within 24 hours after the occurrence of the 2010 Jiasian mainshock.

(Fig. 1). These two fault planes have significantly different tectonic implications. If the causative fault plane strikes in N-S direction, this direction would be consistent with that of the CCF. However, in case that the NW-SE striking plane is the causative fault, its strike direction would be significantly different from that of the CCF and the principle structural orientation of the Taiwan orogenic belt at  $N20^\circ E$ , which would imply the existence of a yet undiscovered structure.

The focal depth of the Jiasian earthquake is also controversial. The focal depths obtained from focal mechanisms of waveform modeling range from 18 to 28 km (CWB: 18 km; BATS: 18 km; GCMT: 27.8 km) and exhibit significant discrepancies from 5 km depth as indicated by the CWB rapid reporting system. This causes the debate concerning the mechanism of observed surface ruptures. If the focal depth of the Jiasian earthquake is located at around 20 km, the event could have been produced by a blind fault and the rupture might have not broken the surface by considering the size of the event. Thus, in order to solve these issues, a better determination of earthquake relocation and focal mechanism is necessary.

Precise earthquake locations rely on several factors, such as record quality, station coverage, adopted methodology of relocation, and the velocity model. The TSMIP stations, which consist of about 800 free-field stations spreading over the island of Taiwan (Shin et al. 2003) are densely distributed over the Jiasian earthquake source region (Fig. 1). The records of the TSMIP stations offer a good opportunity to study this event. For earthquake relocation, we combined the data from CWBSN and TSMIP to obtain a larger dataset and used a 3D velocity model (Wu et al. 2007, 2009a, b). This dataset is also used to perform first-motion focal mechanism determinations to compare with the results of using waveform modeling method. Distributions of PGA and PGV determined from the records of TSMIP are also reported in this study (Fig. 2).

## 2. DATA AND ANALYSIS

The earthquake data used in this study are from two seismic networks: CWBSN and TSMIP. The CWBSN consists of 71 stations equipped with three-component short-period S13 seismometers and is responsible for routine monitoring of regional seismicity in Taiwan (Shin 1992, 1993; Fig. 1). In addition to the records from CWBSN, we further included the P arrivals, S arrivals, S-P times, and the P-arrival polarities from TSMIP to relocate the Jiasian earthquake sequence and to determine the first-motion focal mechanisms. These additional TSMIP stations with an average station spacing of about 5 km except the high-mountain regions significantly greatly improve the stations coverage and the determination of Jiasian earthquake epicenter. Finally, 7905 P arrivals, 6322 S arrivals, 419 S-P times, and 1417 P-arrival polarities from 373 stations were

used in this study (Fig. 1).

A total of 953 aftershocks following the Jiasian mainshock in a period of 43 days were recognized based on temporal and spatial double-link clustering analysis (Wu and Chiao 2006). The linking parameters in time and space are 1 day and 5 km, respectively. Most of the aftershocks occurred within 24 hours after the Jiasian mainshock and were confined to the earthquake source region. Thus, a total of 474 aftershocks occurred within 24 hours were selected for analysis to investigate the causative fault geometry.

The study region is located in Pingtung region with a large lateral variation in the crustal velocity structure (Wu et al. 2007). In order to obtain a good result, we adopted a 3DCOR program proposed by Wu et al. (2003b) for earthquake relocation. It is modified from the 3D location method published by Thurber and Eberhart-Phillips (1999), in which theoretical travel times of P and S are calculated by 3D ray-tracing (Thurber 1993). A three-dimensional velocity model (Wu et al. 2009b) was used instead of the one-dimensional velocity model used in CWBSN location algorithm (Chen 1995). After earthquake relocation, we applied the genetic search algorithm, FPsearch (Wu et al. 2008a), to determine the first motion focal mechanisms using. This method provides a quality index,  $Q_{fp}$ , to measure if the solution is good.  $Q_{fp} = 0$  is a non-constraint solution, and  $Q_{fp} > 1$  is generally considered as a good solution. To the end, a total of 16 focal mechanism solutions of which  $Q_{fp} > 1$  were determined in this study (Table 1).

## 3. RESULTS

### 3.1 Distribution of the Relocated Aftershocks and Focal Mechanisms

Figure 3 illustrates the distribution of first-motion polarities of P waves of the mainshock in the lower-spherical projection. A total of 362 polarities collected from CWBSN and TSMIP provided us a much denser coverage to better constrain the fault plane. The resulting focal mechanism we obtained is quite robust with a minor misfit of 5.73%, a large  $Q_{fp}$  of 5.37, and small deviation of its strike, dip, and rake within  $4^\circ$  (Wu et al. 2008a). The maximum and minimum principal stress axes ( $\sigma_1$  and  $\sigma_3$ ) are orientated in the azimuth of  $256^\circ$  and  $144^\circ$  with plunges of  $13^\circ$  and  $58^\circ$ , respectively. When we compared these results with results from GCMT, BATS, and CWB, they are roughly consistent (Fig. 1). Figure 4 shows the distribution of relocated Jiasian earthquake sequence and first-motion focal mechanisms of selected aftershocks. In general, the distribution of the relocated aftershocks has a linear pattern trending roughly NW-SE. Based on the distribution of aftershocks, the nodal plane with strike  $313^\circ$ , dip  $41^\circ$ , and rake  $42^\circ$  (nodal plane B in Fig. 3) is the more plausible fault plane, with a combination of the southwestward thrusting and left-lateral strike-slip components.

Table 1. Parameters of focal mechanisms determined in this study. The number (No.) of an event represents the temporal order at which the earthquake occurred during the Jiasian earthquake sequence.

No.	Date	Time	Longitude (deg.)	Latitude (deg.)	Depth (km)	$M_L$	Strike (deg.)	Error (deg.)	Dip (deg.)	Error (deg.)	Rake (deg.)	Error (deg.)	$Q_p^*$
1	2010/3/4	00:18:52	120.699	22.962	23.2	6.4	188	±4	64	±3	122	±4	5.37
2	2010/3/4	00:24:47	120.614	22.978	18.7	4.7	168	±2	70	±7	125	±8	4.63
3	2010/3/4	02:30:42	120.605	22.968	16.1	3.8	191	±11	72	±22	143	±29	2.01
4	2010/3/4	02:32:36	120.661	22.958	19.8	3.9	199	±9	87	±22	143	±34	1.78
5	2010/3/4	02:43:36	120.598	22.969	15.5	3.7	14	±7	65	±14	150	±14	1.68
6	2010/3/4	02:48:34	120.598	22.975	16.2	3.8	180	±2	68	±14	129	±13	2.69
7	2010/3/4	04:01:59	120.634	22.955	17.8	3.8	10	±6	76	±16	176	±51	1.62
8	2010/3/4	05:24:09	120.587	23.003	14.4	3.8	187	±16	27	±10	138	±27	2.55
9	2010/3/4	06:30:31	120.648	22.953	18	3.7	186	±9	76	±16	143	±32	1.22
10	2010/3/4	08:07:59	120.613	22.968	16.8	4.4	199	±2	63	±5	160	±15	5.68
11	2010/3/4	08:16:16	120.629	22.954	19.2	5.7	194	±1	64	±2	148	±3	7.12
12	2010/3/4	08:27:18	120.649	22.951	17.7	4.3	200	±6	88	±22	146	±32	2.14
13	2010/3/4	09:47:03	120.621	22.951	17.6	4.3	196	±5	57	±7	155	±8	7.28
14	2010/3/4	10:31:26	120.651	22.960	17	3.7	182	±6	79	±16	160	±36	1.96
15	2010/3/4	12:09:14	120.694	22.942	19	3.7	178	±9	76	±25	169	±35	3.28
16	2010/3/4	16:05:58	120.564	23.004	16.6	4	184	±7	70	±5	118	±5	6.54

\*Quality factor given by Wu et al. (2008a).

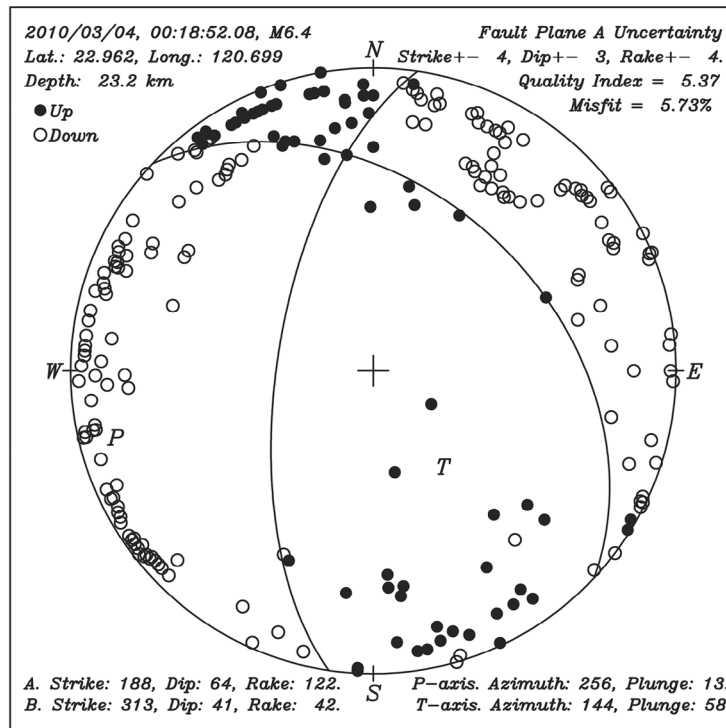


Fig. 3. The lower spherical projection of the first-motion polarities of the Jiasian earthquake. A total of 362 polarities collected from CWBSN and TSMIP are used to determine the focal mechanism.

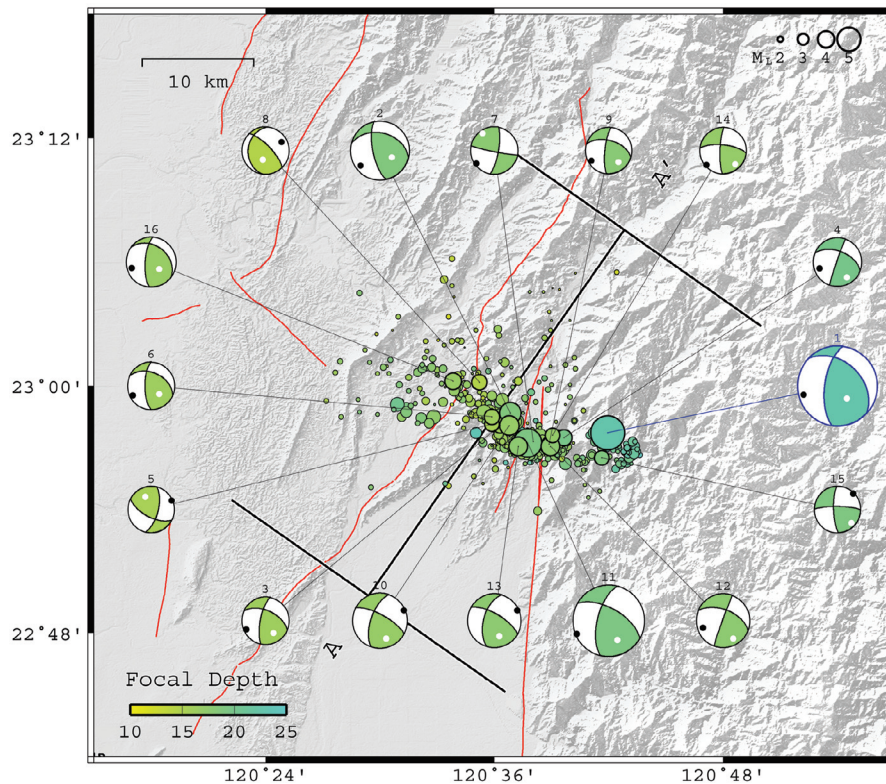


Fig. 4. Distributions of the relocated Jiasian earthquake sequence and focal mechanisms. The numbers above the beach balls represent the temporal order of their occurrence, as in Table 1, and the sizes of the beach balls are proportional to the magnitude. Line AA' is the location of the cross section showed in Fig. 5. The color bar reflects the variation of the focal depth. Red lines are the active fault traces published by Central Geological Survey (CGS).

The focal mechanisms of the aftershocks, in general, are similar to that of the mainshock, but with a much larger strike-slip component and higher dip angles (Fig. 4). The detail parameters of focal mechanisms are listed in Table 1. The index number of a given focal mechanism in Fig. 4 and Table 1 represents the temporal order of which the event occurred. Further exploration of the temporal occurrence order reveals a tendency of rupture propagation from East to West repeatedly, e.g., No. 1 - 3 and No. 4 - 6, before the occurrence of the largest aftershock, No.11.

Figure 5 shows the hypocenter distribution of the relocated aftershocks and the focal mechanisms for  $M \geq 4.0$  events along the profile A - A' (the location is shown in Fig. 4). Most of the aftershocks were located within the range between 10 and 25 km in depth. Northeastward dipping of the aftershocks distribution is consistent with the previously mentioned more possible fault plane (nodal plane B in Fig. 3). It seems that the rupture initiated with the mainshock at the deeper part and propagated toward the shallower part, but was limited at a depth of ca. 10 km. The dipping angle of the plane exhibits a change from gentle at deep part to steep at shallow part, which is similar to the case of the 2003 Chengkung earthquake (Wu et al. 2006).

### 3.2 Distribution of PGA and PGV

Figure 2 shows the distributions of PGA and PGV obtained from TSMIP records. During the earthquake, the maximum PGA can reach up to 475 gal around the epicenter area (recorded by the station MTN154) and propagate outward along a NWW-SEE trend to Chiayi and adjacent areas (Fig. 2a). This trend is roughly parallel with the relocated earthquake sequence. The NWW-SEE trending pattern can be observed more clearly in the PGV distribution (Fig. 2b). In the PGV distribution, the larger values are mainly located to the west and northwest of the epicenter area.

## 4. DISCUSSION

### 4.1 Is the Chaochou Fault the Causative Fault?

The CCF was initially considered as the causative fault of the Jiasian earthquake due to its proximity to the epicenter and the shallow focal depth of the event. From our earthquake relocation and focal mechanism determinations, this sequence shows a NWW-SEE trending distribution and a NNE-dipping fault plane with thrust and left-lateral strike-slip components (Figs. 4 and 5). This NWW-SEE striking

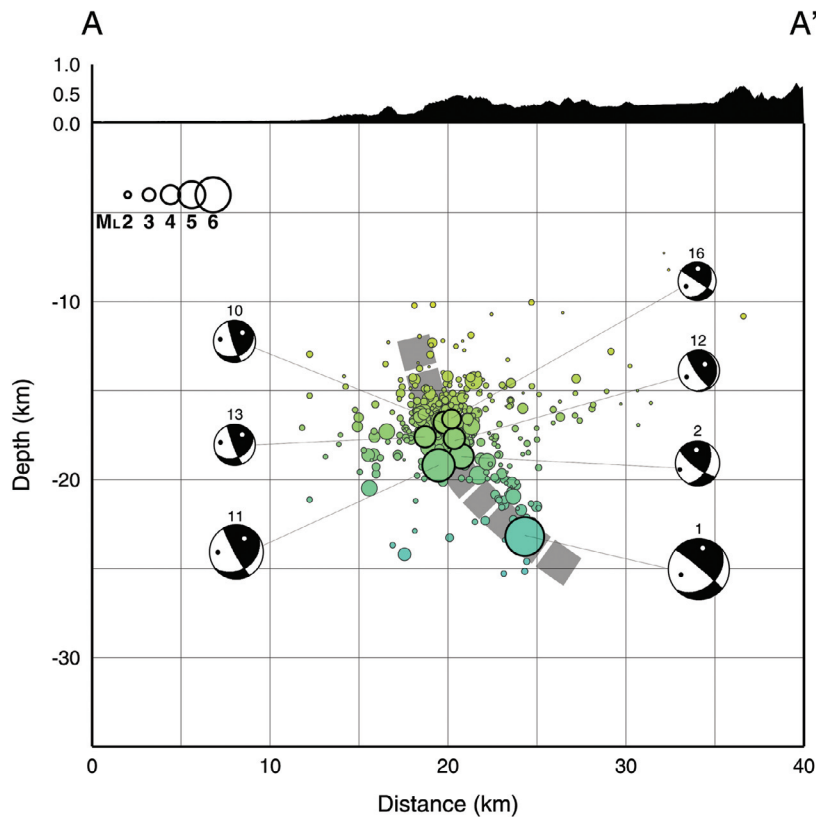


Fig. 5. Cross section of the Jiasian earthquake sequence (showed as line AA' in Fig. 4). Focal mechanisms of  $M_L \geq 4.0$  earthquakes are plotted. The numbers above the beach balls represent the temporal order of their occurrence, and the sizes of the beach balls are proportional to the magnitude. The dashed gray line is the possible fault geometry.

of the causative fault is significantly different from the N-S striking of the CCF. This suggests that the Jiasian earthquake is quite unlikely to be produced by the rupture of the CCF.

Furthermore, according to earlier surveys by the Chinese Petroleum Corporation (CPC) (Yen and Tien 1986), the CCF is an east-dipping reverse fault with left-lateral strike-slip components. The movement along this fault could also be demonstrated by the contrast between the rock ages and elevations across the fault (Shyu et al. 2005), as well as the analysis of geomorphic features (Liao 2003). The remarkably straight N-S trending escarpment along the fault suggests the existence of a significant component of strike-slip motion. However, results from geodetic and seismic studies do not show major activity of the fault at present. The velocity gradient across the CCF from dense GPS measurements is not significant (Hu et al. 2007). Also, no earthquake is clearly related to the fault in relocated background seismicity (Wu et al. 2008b). This implies that the CCF could have been active in a longer timescale, but seems to be much less active or even inactive during the seismicity data period, 1991 - 2006. Considering its fault length (Shyu et al. 2005), the CCF might be a potential seismogenic source for a destructive earthquake in the future if it is locked.

#### 4.2 Surface Rupture?

Some ground cracks were immediately noted and reported by Chang et al. (2010) right after the Jiasian mainshock. Hence, whether the causative fault ruptured to the surface becomes another issue. Results from our study show that not only the hypocenter of the Jiasian mainshock is at 23 km deep but almost all the aftershocks are distributed below the depth of 10 km (Fig. 5). This suggests that the causative fault is restricted below 10 km depth. Therefore, the observed surface cracks are likely produced by the dynamic shaking of the ground from the propagating waves, not the actual rupture of the fault.

#### 4.3 Earthquake Hazards Potential in Southern Taiwan

Although the Jiasian earthquake occurred at a deep depth as mentioned previously, it caused strong ground shaking in and around the epicenter area. Especially in the Chiayi region about 60 km away from the epicenter, most of the PGA exceeds 200 gal. If taking this distance and the magnitude of the Jiasian earthquake into account to calculate the empirical PGA and PGV by the attenuation formula of Wu et al. (2001), we obtained a PGA of ca.

46 gal and the PGV of ca.  $5 \text{ cm s}^{-1}$ . This suggests the values of PGA and PGV in the Chiayi region are abnormally high (Fig. 2). According to our proposed focal mechanism of the Jiasian earthquake (Fig. 4), the left-lateral strike-slip component along the NW-SE striking fault plane suggests greater ground motion toward the northwest in the hanging wall area than that in the footwall area such as the Pingtung area, where weaker ground shaking than the hanging wall area were observed at comparable epicentral distances. As indicated in the peak ground motion distributions in Fig. 2 especially for PGV, this northwestward propagating pattern seems to be caused by the directivity effect of the fault rupture direction.

Alternatively, another reason for the stronger PGA and PGV recorded in the Chiayi region could be the site effect. Previous studies (e.g., Lee et al. 2001; Wu et al. 2001; Huang 2009) showed that the site condition in the Chiayi region is classified as the soft-soil condition and is capable of producing large site amplification. Therefore, the sediments underneath the Chiayi region can intensify the ground shaking once the seismic waves propagate to the Chiayi Plain area. Since the Chiayi region is highly populated, the fault or the seismogenic zone revealed by the 2010 Jiasian earthquake should be considered in future regional seismic hazard assessments.

The 2010 Jiasian earthquake also demonstrated an urgent need for a short-distance earthquake early warning (EEW) system for urban areas in southern Taiwan. Wu et al. (2011) tested a short-distance EEW approach for the 2010 Jiasian earthquake, which is a threshold-based approach using continued monitoring of filtered vertical displacements. They showed that the tested short-distance EEW approach can provide a timely warning for the target sites located less than 50 km away from the epicenter.

## 5. CONCLUSIONS

This study aims to clarify the locations and the focal mechanisms of the 2010 Jiasian earthquake sequence and to interpret the tectonic significance revealed by this event. By integrating the data from CWBSN and TSMIP, we are able to obtain more reliable results. Our results show that the Jiasian earthquake is located at the depth of 23 km, instead of the original reported depth of 5 km by the CWB rapid reporting system. With the help of relocated aftershock distributions, we believe the first-motion focal mechanism has a more plausible plane of strike  $313^\circ$ , dip  $41^\circ$ , and rake  $42^\circ$ . This causative fault plane is significantly different from the N-S striking CCF, as well as the principal trend of structures in the Taiwan orogenic belt. The focal mechanisms of aftershocks are mostly consistent with this causative fault plane.

Based on this deep focal depth and the NW-SE striking fault plane, the Jiasian earthquake was probably pro-

duced by rupture on an undiscovered fault, rather than the CCF. The limited aftershock focal depths of deeper than 10 km also suggest that this fault is a deep blind fault that did not rupture to the surface. Therefore, the observed surface cracks are likely produced by dynamic ground shaking, not the actual rupture movement. Moreover, our analysis of the PGA and PGV distributions provides insight into the future seismic hazards in the Chiayi area and adjacent regions. Due to the directivity and site effects, a similar type of rupture in the Jiasian area would likely cause strong ground shaking in the Chiayi region as the seismic waves propagating northwestward. This observation will have important implications for the hazard assessments in the future.

**Acknowledgements** This work was supported by the National Science Council (NSC99-2119-M-002-022, NSC99-2627-M-002-015, NSC98-3114-M-002-001) and Central Weather Bureau. The software package GMT (Wessel and Smith 1998) was used in this study and is gratefully acknowledged. The authors also thank Central Weather Bureau for providing seismic data used in this study.

## REFERENCES

- Chang, C. P., W. H. Chang, C. H. Hou, Y. C. Liu, and K. F. Ma, 2010: The relationship between the NE-SW striking structures in the mountain regions and the Jiasian earthquake, southwestern Taiwan. Annual Congress of Chinese Geophysical Society and the Geological Society of Taiwan, Abstract. (in Chinese).
- Chen, Y. L., 1995: A study of 3-D velocity structure of the crust and the subduction zone in the Taiwan region. Master Thesis, National Central University, Jhongli, Taiwan, 172 pp. (in Chinese)
- Hu, J. C., C. S. Hou, L. C. Shen, Y. C. Chan, R. F. Chen, C. Huang, R. J. Rau, K. H. H. Chen, C. W. Lin, M. H. Huang, and P. F. Nien, 2007: Fault activity and lateral extrusion inferred from velocity field revealed by GPS measurements in the Pingtung area of southwestern Taiwan. *J. Asian Earth Sci.*, **31**, 287-302, doi: 10.1016/j.jseaes.2006.07.020. [[Link](#)]
- Huang, J. Y., 2009: Using microtremor measurement to study the site effect in Taiwan area. Master Thesis, National Central University, Jhongli, Taiwan, 240 pp. (in Chinese)
- Lee, C. T., C. T. Cheng, C. W. Liao, and Y. B. Tsai, 2001: Site classification of Taiwan free-field strong-motion stations. *Bull. Seismol. Soc. Am.*, **91**, 1283-1297, doi: 10.1785/0120000736. [[Link](#)]
- Liao, H. S., 2003: Research of active structures along the Chaochou Fault in the southern Taiwan by geomorphic index. Master Thesis, National Central University, Chungli City, Taiwan, 124 pp. (in Chinese)
- National Fire Agency News Release, 2010: The case of

- the  $M_L = 6.4$  earthquake at a distance 17 km southeast away from the Jiasian seismic station.
- Shin, T. C., 1992: Some implications of Taiwan tectonic features from the data collected by the Central Weather Bureau Seismic Network. *Meteorol. Bull.*, **38**, 23-48. (in Chinese)
- Shin, T. C., 1993: Progress summary of the Taiwan strong motion instrumentation program. In: Proceeding of Symposium on Taiwan Strong Motion Instrumentation Program, Central Weather Bureau, Taipei, Taiwan, 1-10. (in Chinese)
- Shin, T. C., Y. B. Tsai, Y. T. Yeh, C. C. Liu, and Y. M. Wu, 2003: Strong-motion instrumentation programs in Taiwan. In: Lee, W. H. K., H. Kanamori, P. C. Jennings, and C. Kisslinger (Eds.), *Earthquake and Engineering Seismology*, Academic Press, San Diego, 1057-1062.
- Shyu, J. B. H., K. Sieh, Y. G. Chen, and C. S. Liu, 2005: Neotectonic architecture of Taiwan and its implications for future large earthquakes. *J. Geophys. Res.*, **110**, B08402, doi: 10.1029/2004JB003251. [[Link](#)]
- Thurber, C. H., 1993: Local earthquake tomography: Velocities and  $V_p/V_s$ -theory. In: Iyer, H. M. and K. Hirahara (Eds.), *Seismic Tomography: Theory and Practice*, Chapman & Hall, London, UK.
- Thurber, C. and D. Eberhart-Phillips, 1999: Local earthquake tomography with flexible gridding. *Comput. Geosci.*, **25**, 809-818, doi: 10.1016/S0098-3004(99)00007-2. [[Link](#)]
- Wessel, P. and W. H. F. Smith, 1998: New, improved version of generic mapping tools released. *Eos, Trans., AGU*, **79**, 579, doi: 10.1029/98EO00426. [[Link](#)]
- Wu, Y. M. and L. Y. Chiao, 2006: Seismic quiescence before the 1999 Chi-Chi, Taiwan,  $M_w$  7.6 earthquake. *Bull. Seismol. Soc. Am.*, **96**, 321-327, doi: 10.1785/0120050069. [[Link](#)]
- Wu, Y. M., T. C. Shin, C. C. Chen, Y. B. Tsai, W. H. K. Lee, and T. L. Teng, 1997: Taiwan rapid earthquake information release system. *Seismol. Res. Lett.*, **68**, 931-943.
- Wu, Y. M., T. C. Shin, and C. H. Chang, 2001: Near real-time mapping of peak ground acceleration and peak ground velocity following a strong earthquake. *Bull. Seismol. Soc. Am.*, **91**, 1218-1228, doi: 10.1785/0120000734. [[Link](#)]
- Wu, Y. M., N. C. Hsiao, T. L. Teng, and T. C. Shin, 2002: Near real-time seismic damage assessment of the rapid reporting system. *Terr. Atmos. Ocean. Sci.*, **13**, 313-324.
- Wu, Y. M., T. L. Teng, T. C. Shin, and N. C. Hsiao, 2003a: Relationship between peak ground acceleration, peak ground velocity, and intensity in Taiwan. *Bull. Seismol. Soc. Am.*, **93**, 386-396, doi: 10.1785/0120020097. [[Link](#)]
- Wu, Y. M., C. H. Chang, N. C. Hsiao, and F. T. Wu, 2003b: Relocation of the 1998 Ruyli, Taiwan, earthquake sequence using three-dimensions velocity structure with stations corrections. *Terr. Atmos. Ocean. Sci.*, **14**, 421-430.
- Wu, Y. M., Y. G. Chen, T. C. Shin, H. Kuochen, C. S. Hou, J. C. Hu, C. H. Chang, C. F. Wu, and T. L. Teng, 2006: Coseismic versus interseismic ground deformations, fault rupture inversion and segmentation revealed by 2003  $M_w$  6.8 Chengkung earthquake in eastern Taiwan. *Geophys. Res. Lett.*, **33**, L02312, doi: 10.1029/2005GL024711. [[Link](#)]
- Wu, Y. M., C. H. Chang, L. Zhao, J. B. H. Shyu, Y. G. Chen, K. Sieh, and J. P. Avouac, 2007: Seismic tomography of Taiwan: Improved constraints from a dense network of strong motion stations. *J. Geophys. Res.*, **112**, B08312, doi: 10.1029/2007JB004983. [[Link](#)]
- Wu, Y. M., L. Zhao, C. H. Chang, and Y. J. Hsu, 2008a: Focal-mechanism determination in Taiwan by genetic algorithm. *Bull. Seismol. Soc. Am.*, **98**, 651-661, doi: 10.1785/0120070115. [[Link](#)]
- Wu, Y. M., C. H. Chang, L. Zhao, T. L. Teng, and M. Nakamura, 2008b: A comprehensive relocation of earthquakes in Taiwan from 1991 to 2005. *Bull. Seismol. Soc. Am.*, **98**, 1471-1481, doi: 10.1785/0120070166. [[Link](#)]
- Wu, Y. M., L. Zhao, C. H. Chang, N. C. Hsiao, Y. G. Chen, and S. K. Hsu, 2009a: Relocation of the 2006 Pingtung earthquake sequence and seismotectonics in Southern Taiwan. *Tectonophysics*, **479**, 19-27, doi: 10.1016/j.tecto.2008.12.001. [[Link](#)]
- Wu, Y. M., J. B. H. Shyu, C. H. Chang, L. Zhao, M. Nakamura, and S. K. Hsu, 2009b: Improved seismic tomography offshore northeastern Taiwan: Implications for subduction and collision processes between Taiwan and the southernmost Ryukyu. *Geophys. J. Int.*, **178**, 1042-1054, doi: 10.1111/j.1365-246X.2009.04180.x. [[Link](#)]
- Wu, Y. M., T. L. Lin, W. A. Chao, H. H. Huang, N. C. Hsiao, and C. H. Chang, 2011: Faster short-distance earthquake early warning using continued monitoring of filtered vertical displacement: A case study for the 2010 Jiasian, Taiwan, earthquake. *Bull. Seismol. Soc. Am.*, **101**, 701-709, doi: 10.1785/0120100153. [[Link](#)]
- Yen, T. P. and P. L. Tien, 1986: Chaochou fault in Southern Taiwan. *Proc. Geol. Soc. China*, **29**, 9-22.